Volume 1, Issue 2 – July – December – 2017

ECORFAN

Journal-Taiwan

ISSN-ON line 2524-2121

ECORFAN®

Indexing

Academic Google

ECORFAN® Taiwan

ECORFAN Journal-Taiwan, Volume 1, Issue 2, July-December 2017, is a journal edited semestral by ECORFAN ECORFAN-Taiwán. Taiwan, Taipei. YongHe district, ZhongXin, Street 69. Postcode: 23445. WEB: www.ecorfan.org/taiwan/,journal@ecorfan.org. Editor in Chief: RAMOS-ESCAMILLA, María. ISSN: 2524-2121. Responsible for the latest update of this number ECORFAN Computer Unit.Escamilla Bouchán-Imelda, Luna Soto-Vladimir, last updated December 31, 2017.

Editorial Board

Arbitration Committee

BMC. PhD.
Universidad Industrial de Santander, Colombia

BMLF. PhD.
Universidad de Concepción, Chile

RAG. PhD.
University of Iowa, USA

VMC. PhD.
Universidad de Guanajuato, México

RLR. PhD.
Universidad de Guanajuato, México

ASG. PhD
Universidad Autónoma del Estado de Morelos

MELO. PhD.
Universidad Autónoma de San Luis Potosí, México

GRMA. PhD
Universidad de Guadalajara, Mexico

TANI. PhD.
Centro de Investigaciones en Optica, México

JVD. PhD.
Universidad de Guanajuato, México

Presentation

ECORFAN Journal-Republic of Taiwan is a research journal that publishes articles in the areas of:

Applied Optics

In Pro-Research, Teaching and Training of human resources committed to Science. The content of the articles and reviews that appear in each issue are those of the authors and does not necessarily the opinion of the editor in chief.

In Number 1st presented the article Optical characterization of nanostructured opal-C by DURÁN-MUÑOZ, H. A., SIFUENTES-GALLARDO, C., HERNÁNDEZ-ORTIZ, M., DÍAZ-CARRILLO, C., ULLOA-CAMPOS, M., ORTIZ-HERNÁNDEZ, A. and GUTIÉRREZ-ALMARAZ, G. with adscription in Universidad Autónoma de Zacatecas and Universidad Politécnica de Zacatecas, the next article name is Optical method to measure peroxides: A setup for edible oils sensing using a core-offset Mach-Zehnder Interferometer by CUCHIMAQUE-LUGO, Leidy Johanna, SOSA-MORALES, María Elena, CASTRO-LÓPEZ Rafael, ESTUDILLO-AYALA, Julián Moisés, JAUREGUI-VAZQUEZ, Daniel, HERNANDEZ-GARCÍA, Juan Carlos, SIERRA-HERNANDEZ, Juan Manuel, and ROJAS-LAGUNA, Roberto with adscription in Universidad de Guanajuato in the next Section the article Detecting glucose levels by means of Raman spectroscopy, support vector machine and principal component analysis by CASTRO-RAMOS, J., VILLA-MANRÍQUEZ, J. F., GÓMEZ-GIL, P., GONZÁLEZ-VIVEROS, N., NAREA-JIMÉNEZ, F., SÁNCHEZ-ESCOBAR J. J., and MUÑOZ-LÓPEZ, J., adscripted on Instituto Nacional de Astrofísica Óptica y Electrónica and Centro de Enseñanza Técnica Industrial and the article Sugar concentration sensor based on a micro fabry-perot interferometer by GUZMAN-CHAVEZ, Ana Dinora, CANO-CONTRERAS, Martín and JAUREGUI-VAZQUEZ, Daniel, adscripted in Universidad de Guanajuato and Universidad Tecnológica del Suroeste de Guanajuato.

Content

Article **ECORFAN-Journal**
December 2017 Vol.1 No.3 1-5

Optical characterization of nanostructured opal-C

DURÁN-MUÑOZ, H. A.†[']', SIFUENTES-GALLARDO, C.[']', HERNÁNDEZ-ORTIZ, M.[']', DÍAZ-CARRILLO, C.[¨], ULLOA-CAMPOS M.[¨], ORTIZ-HERNÁNDEZ A and GUTIÉRREZ-ALMARAZ G.''

[']*Universidad Autónoma de Zacatecas, Departamento de Ingeniería Eléctrica, Av. Ramón López Velarde 801. Col. Centro, C.P. 98000. Zacatecas, Zac., México.*
[¨]*Universidad Politécnica de Zacateca, Carrera de Ingeniería Industrial. Plan del Pardillo S/N, Parque Industrial, Fresnillo, Zac. México.*

Received: September, 8, 2017; Accepted: December, 15, 2017

Abstract

The emission of light from a thermally stimulated solid is called thermoluminescence (TL). The TL technique is a useful tool to characterize defects in materials.The aim of this work is realize a complementary TL study of synthetic opal-c reported on literature (Hernández-Ortiz *et. al.*, 2015; Hernández-Ortiz *et. al.*, 2012; Hernández-Ortiz *et. al.***,** 2013), determining the kinetic parameters, which can be useful for photo transference applications, studies on defect creation, etc. Opal-C nanoparticles were synthesized by Stöber method. TL measurements of opal-c nanoparticles were carried out at room temperature using an automated Risø TL/OSL system model TL DA-20. Also, the Mckeever experiment was performed in order to know the peaks distribution, and was used a friendly glow curve deconvolution spreadsheet based on general order kinetic equation as a complementary technique to determine the kinetic parameters. Therefore, it is possible to carry out another level of synthetic Opal-C study, either to apply it in the medical sector, dosimetry, photo-transfer studies, archaeological dating, etc.

Thermoluminescence, Glow Curve Deconvolution and Opal-C Nanoparticles

Citation: DURÁN-MUÑOZ, H A†, SIFUENTES-GALLARDO, C, HERNÁNDEZ-ORTIZ, M, DÍAZ-CARRILLO, C, ULLOA-CAMPOS, M, ORTIZ-HERNÁNDEZ, A and GUTIÉRREZ-ALMARAZ, G. Optical characterization of nanostructured opal-C. ECORFAN Journal-Taiwan. 2017, 1-2: 1-5

† Researcher contributing as first author.

Introduction

The humanity is exposed directly and indirectly to opal, for example, some animals and plants contain opal as a cross-linking agent in a natural hydrated silica, with a crystal structure connective tissues (Iler, 1955 and 1979), and it is commonly used as semiprecious stone. Opal is type fcc and a direction [111] as the preferred orientation (Hernández-Ortiz *et. al.,* 2015; Golubev *et. al.,* 2002), and can be subdivided into three well defined structural groups: opal-CT, where the stacking sequence is apparently about 50% cristobalite and 50 % tridymite, and it is typically of volcanic origin (Hernández-Ortiz *et. al.,* 2012-B), it gives an X-ray diffraction pattern with markedly broad reflections, approximately at the positions of the strong lines of cristobalite; opal-C approximately 80 to 70% cristobalitic and 20 to 30% tridymitic; which is a well ordered form of the silicate and exhibit play-of-color of common opal (Jones and Segnit, 1971); play-of-color or noble opal is most known as opal-A (for amorphous), which is generally of sedimentary origin and it was found that there were anomalies in the relationship between water and hydroxyl content and certain physical properties, its classical localities are Australia and the Piaui State of Brazil (Graetsch *et. al.,* 1994; Fritsch *et. al.,* 2006).

Opal synthetic has a wide range of applications in different areas of knowledge, due to the ability to control the dimensions of the particle size; different particle sizes are required for different applications (Rossi *et. al.,* 2005). For example, silica nanoparticles, viewed as photonic crystal, are being developed as a host of biotechnological applications; one of them is the infiltration of biomolecules in photonic crystals to get improved luminescence spectra of DNA due to the possible formation of new photon-electron bound states.

Also, it is used on characterization of photonic materials performed by scattering matrix method (Reynolds *et. al.,* 1999). Recently, it has been proposed in dosimetry applications, due to bio-compatibility properties and an adequate response at high doses (Hernández-Ortiz *et. al.,* 2015; Hernández-Ortiz *et. al.,* 2012; Hernández-Ortiz *et. al.,* 2013).

However, an additional TL characterization on synthetic opal-C is necessary to perform. In order to characterize the defects associated to the overlapped peaks in a glow curve (electrical signal generated by TL technique). Each overlapped peak has peak parameters, I_m: maximum intensity of each peak, T_m: temperature in the maximum intensity and *w*: width of peak. Also, each defect has trap parameters, E: activation energy, *s*: frequency factor, b: order of kinetic and n_a: concentration of electron trapped. With the glow curve deconvolution technique, it is possible to obtain the trap and peak parameters.

The aim of this work is realize a complementary thermoluminescence charaterization of synthetic opal-c reported on literature, determining the kinetic parameters, which can be useful in next works for photo transference applications, studies on defect creation, etc.

Methodology

In this work were used synthetic Opal-C samples, which were synthesized by Stöber method, consisting in the hydrolysis of tetraethyl-ortho-silicate (TEOS) using NH_3 as a catalyst and ethanol and acetone as solvent. The reaction was controlled in a Nalgene glass flask at room temperature. Synthetic opals underwent two thermal treatments aimed at strengthening the structure.

ISSN: 2524-2121

First annealing was fixed at 1000 °C for one day and second thermal treatment was given at 1150 °C for two days. According to the report of Beganskienė, the solution (TEOS, NH_3, H_2O and solvent) chemistry controls the reaction rate and particle size. The powdered samples were obtained by crushing the synthesized opal-c using an agate pestle. Then, TL measurements of opal-c nanoparticles were carried out at room temperature (~22 ºC) using an automated Risø TL/OSL system model TL DA-20 equipped with a ^{90}Sr source beta (Figure 1) which delivers a 5 Gy min^{-1} dose rate. All the TL measurements were performed using a linear heating rate of 5 ºC s^{-1} from 22 ºC up to 510 ºC, in an N_2 atmosphere.

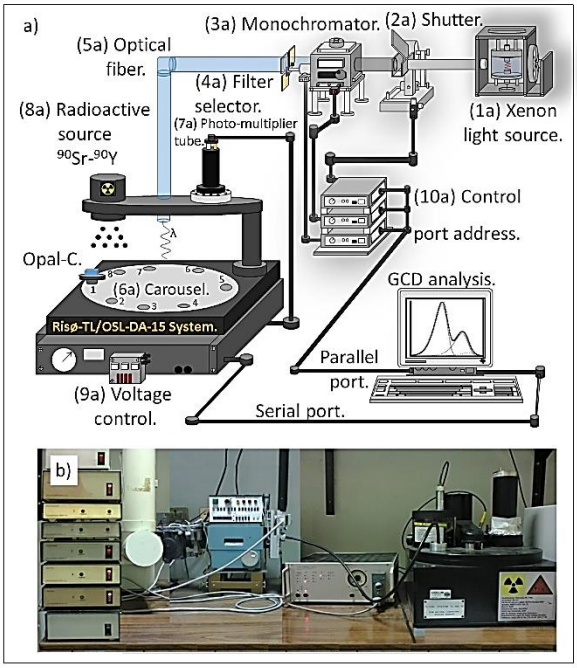

Figure 1. a) Diagram and d) experimental setup of luminescence system.

After of excitation, the carousel of Risø-TL/OLS-DA-15 system (Figure 1, 6a) is rotated to place the crystal below the photo-multiplier tube (Figure 1, 7a), and start a thermal stimulation producing light emission, which is detected with the photomultiplier tube.

The signal is processed by the computer and is represented as a glow curve. Finally, the Mckeever experiment was performed with a thermal cleaning of $\Delta T = 5$ ° (T_{Stop}). Also, a friendly glow curve deconvolution spreadsheet (GCDS) based on general order kinetic equation was used as complementary technique to determine the kinetic parameters. This GCDS has been used to characterize other materials.

Results and Discussions

The Mckeever experiment (Figure 2) reveals 3 ranges of emission, around of 50-270, 275-350 and 355-510 °C.

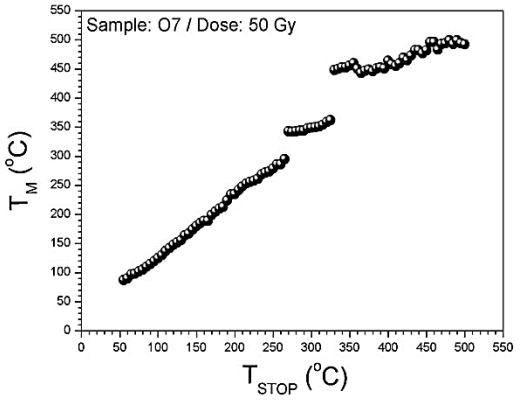

Figure 2. Mckeever experiment graph (T_M-T_{STOP}), Opal-c sample exposed a dose of 50 Gy.

In the first temperature range (50-270 ° C), 4 overlapped peaks are associated (1-4, Table 1), with activation energy very close to each other. These values support the hypothesis that the quasi-continuous distribution of traps occurs in this temperature range. In the second temperature range (275-350 °C), 2 overlapped peaks are associated (5-6, Table 1), with kinetic order values different from 1, which is supported by Mckeever experiment (Figure 2).

In the third temperature range (355-510 °C), 2 overlapped peaks are associated (7-8, Table 1), with a large peak width and a kinetic of second order.

ISSN: 2524-2121

Using the GCDS, reported for the characterization of other materials (Muñoz ***et. al.,*** 2014; Sánchez-Zeferino ***et. al.,*** 2013), it was possible identify the overlapped peaks in the experimental glow curve (Figures 3 and 4).

Using the simultaneously numerical fitting proposed in this work, it is possible to have evidence that the overlapped peaks obtained are associated with real values of the material.

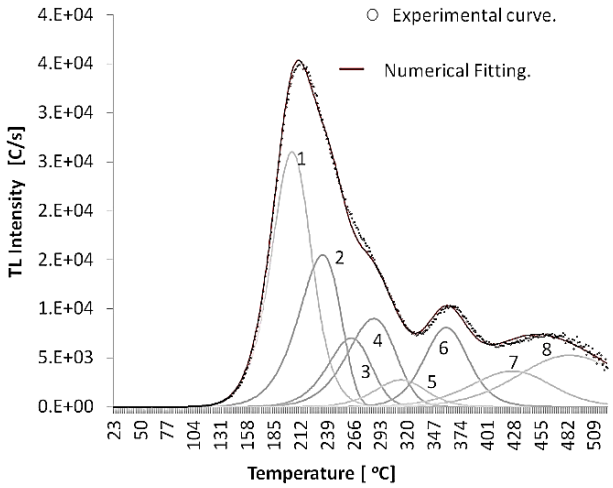

Figure 3. Glow curve deconvolution with a thermal treatment of 80 °C.

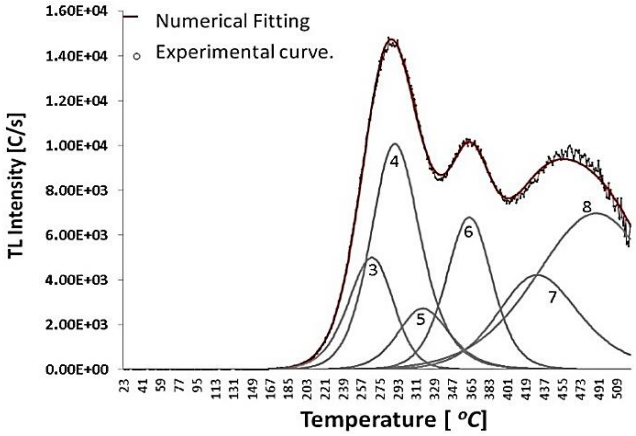

Figure 4. Glow curve deconvolution with a thermal treatment of 150 °C.

The simultaneously glow curve deconvolution process generates a FOM value (Figure of Merit) of 2.18. Normally, a FOM value below 5 is considered a good numerical fitting. The trap and peak parameters are presented in Table 1, with these parameters it is possible to identify the trapping states of opal-c.

Peaks	T_m [°C]	I_m [arb. u.]	*w*	E [eV]	s [s^{-1}]	*b*
1	189	26041	46	1.1	5.47E+11	1.6
2	220	15497	51	1.0	1.57E+09	1.0
3	249	7035	50	1.2	6.04E+10	1.3
4	271	9020	56	1.1	5.41E+09	1.2
5	299	2762	59	1.3	1.35E+11	1.6
6	345	8106	51	1.9	1.77E+15	1.8
7	411	3666	94	1.2	4.14E+07	1.5
8	469	5258	135	1.2	7.41E+06	2.0

Table 1. Peak and trap parameters.

Conclusions

In this work the trap and peak parameters of Opal-C are presented for the first time. So, it is possible in other works to take to another level of the study of Synthetic Opal-C, either to apply it in the medical sector, for dosimetric, for studies of photo-transference, archaeological dating, etc. Particularly, The Mckeever experiment (Figure 1) reveals 3 ranges of emission, 50-270, 275-350 and 355-510 °C.

The peaks on low temperatures are generated by the quasi-continuous distribution of traps; while the other peaks correspond to kinetics of order different than 1 or general order. The results of this work serve as a reference for further physical studies.

ISSN: 2524-2121

Acknowledgements

The authors gratefully acknowledge the financial support for this work from PRODEP.

References

Boyko V., Dovbeshko G., Fesenko O., Gorelik V., Moiseyenko V., Romanyuk V., Shvets T. and Vodolazkyy P. (2011). *Mol. Cryst. Liq. Cryst.* 535, pp. 30–41.

Fritsch E., Gaillou E., Rondeau B., Barreau A., Albertini D. and Ostroumov M. (2006). *Journal of Non-Crystalline Solids* 352. Pp. 3957-3960.

Graetsch H., Gies H., Topalović I. (1994). *Physics and Chemistry of Minerals* 21, pp. 166-175.

Golubev V.G., Hutchison J.L. and Kosobukin V.A. (2002). *Journal of Non-Crystalline Solids* 1062, pp. 299–302.

Hernández-Ortiz M., Acosta-Torres L.S., Hernández-Padrón G. (2012). *BioMedical Engineering OnLine* 11, pp. 78-87.

Hernández-Ortiz M, Hernández-Padrón G, Bernal R, Cruz-Vázquez C, Vega-González M and Castaño V. (2012-B). *Digest Journal of Nanomaterials and Biostructures* 7(3), pp. 1297 – 1302.

Hernández-Ortiz M., Acosta-Torres L.S., Bernal R., Cruz-Vázquez C., Castaño V.M. (2013). *MRS Fall Proceeding 1530 mrsf12-1530-xx07-4*.

Hernández-Ortiz M, Hernández-Padrón G., Bernal R., Cruz-Vázquez C. and Castaño V. M. (2015). *International Journal of Basic and Applied Sciences* 4 (2), pp. 238-243.

Iler RK. (1955). New York: Cornell University Press.

Iler RK. (1979). New York: Wiley-Interscience.

Jones J.B., Segnit E.R. (1971). *Australian Journal of Earth Sciences* 18, pp. 57-68.

Masalov V., Sukhinina N., Emel'chenko GA. (2011). *Physics of the Solid State* 53. pp. 1135–1139.

Muñoz I., Brown F., Durán-Muñoz H., Cruz-Zaragoza E., Durán-Torres B., Alvarez-Montaño E. (2014). *Journal of Applied Radiation and Isotopes* 90, pp. 58–61.

Reynolds A., López-Tejeira F., Cassagne D., García-Vidal J., Jouanin C. and Sánchez-Dehesa. (1999). *J. Physical Review B.* 60, pp. 11422.

Rossi L., Shi L., Quina F. and Rosenzweig Z. (2005). *Langmuir* 21 pp. 4277-4280.

Sánchez-Zeferino R., Pal U., Meléndrez R., Durán-Muñoz H. and Barboza Flores M. (2013) Dose enhancing behavior of hydrothermally grown Eu-doped SnO2 nanoparticles. *Journal of Applied Physics* 113 pp. 064306.

ISSN: 2524-2121

Article **ECORFAN-Journal**
December 2017 Vol.1 No.2 6-10

Optical method to measure peroxides: A setup for edible oils sensing using a core-offset Mach-Zehnder Interferometer

CUCHIMAQUE-LUGO, Leidy Johanna,[†] SOSA-MORALES, María Elena,[††] CASTRO-LÓPEZ Rafael,[††] ESTUDILLO-AYALA, Julián Moisés,[†] JAUREGUI-VAZQUEZ, Daniel,[†] HERNANDEZ-GARCÍA, Juan Carlos[†], SIERRA-HERNANDEZ, Juan Manuel,[†] and ROJAS-LAGUNA, Roberto[†]*

[†]*Universidad de Guanajuato, Departamento de Ingeniería Electrónica, División de Ingenierías, Campus Irapuato-Salamanca, , Comunidad de Palo Blanco, Salamanca, Gto., C.P. 36885, México.*

[††] *Universidad de Guanajuato, Departamento de Alimentos, División de Ciencias de la Vida, Campus Irapuato-Salamanca, Carretera Irapuato-Silao km 9, Irapuato, Gto. 36500 México.*

Received August 5,2017 ; Accepted December 12, 2017

Abstract

Peroxide value is the index to follow the primary oxidative rancidity in fats and oils. Peroxides increase in fats and oils used for repeated frying. A peroxide sensing setup based in the Mach-Zehnder Interferometer (MZI) was fabricated. The MZI had the connection of three sections of optical fiber of Single Mode Fiber (SMF) implemented by splicing standard single mode fiber segments (SMF, Single Mode fiber) by the technique of misalignment of the fiber axes. A change in the output spectrum was induced by applying different samples of edible oil with different times of usage for repeated frying on the interferometer. Finally, the experimental results showed a sensitivity of 0.80461 nm/meq/kg for edible oils. The sensor fabrication process is very simple and low cost.

Interferometry, Mach- Zehnder, Edible Oil Sensing, Optical Fiber

Citation: CUCHIMAQUE-LUGO, Leidy Johanna, SOSA-MORALES, María Elena, CASTRO-LÓPEZ Rafael, ESTUDILLO-AYALA, Julián Moisés, JAUREGUI-VAZQUEZ, Daniel, HERNANDEZ-GARCÍA, Juan Carlos, SIERRA-HERNANDEZ, Juan Manuel, and ROJAS-LAGUNA, Roberto. Optical method to measure peroxides: A setup for edible oils sensing using a core-offset Mach-Zehnder Interferometer ECORFAN Journal Taiwan. 2017, 1-2: 6-10

*Correspondence to Autor (email: rlaguna@ugto.mx)

Introduction

Although frying is a relatively simple process of immersing the food product in hot oil, it involves different factors that directly affect the rate of oil degradation and the final product properties. Some of these factors are the type of food, degree of saturation of the oil, oil temperature, and frying time, among others (Enriquez-Fernández et al., 2012). In practice, for repeated frying of foods, the oil remains regularly in the fryer for days at high temperatures, which, along with other aspects such as presence of oxygen environment and water from foods being fried, causes alterations to the oil properties (Flores-Álvarez et al., 2012).

The peroxide value indicates the milliequivalents of oxygen in the form of peroxide by kilogram of fat or oil, this peroxide value (PV) is determined according to the Mexican standard (NMX-F-154-SCFI-2010). Its maximum value is 20 meq/kg; otherwise, the fat/oil must be discarded, as peroxides have been recognized as toxic for the human.

Optical fiber sensors have attracted great attentions in the applications of biological, chemical and environmental industries, including the measurements of the liquid level, refractive index (RI), temperature and strain (Li et al., 2012). Compared to other techniques based on the mechanical, chemical and electrical methods, the optical fiber sensors have several advantages, such as electromagnetic immunity, high sensitivity, capability of remote sensing and low cost.

In this paper, a sensing setup based on a core-offset Mach-Zehnder interferometer was achieved by core-offset fusion splicing of a segment of a single mode fiber between two pieces of single-mode fibers.

Taking into account the characteristics of the fiber optics in different applications, this work refers to the sensing of indices of degradation of edible oils based on an interferometer type Mach-Zehnder fiber optic, where the change of edible oil sample over the MZI, the output power spectrum can be measured.

Methodology

Several types of optical sensors have been proposed to develop Mach-Zehnder interferometers as well as there are several ways to fabricate a MZI along a single-mode fiber (SMF). The commonly used method is to induce and recombine the core mode and cladding modes of a SMF by using core-offset splicing (Zhang et al., 2011; Duan et al., 2011). Figure 1 shows the schematic diagram to implement the Mach-Zehnder Interferometer.

The sensor was formed by fusion splicing a section of 6 cm of single-mode fiber (SMF-28) between two sections of single-mode fibers, which functions as a detection sensor for the peroxide levels present when making direct contact with the sample. The core and cladding are considered as the arms of the MZI, while the offset act as optical fiber couples, for this case, the axes of a conventional single-mode fiber (SMF-28) were misaligned by 20 μm (offset).

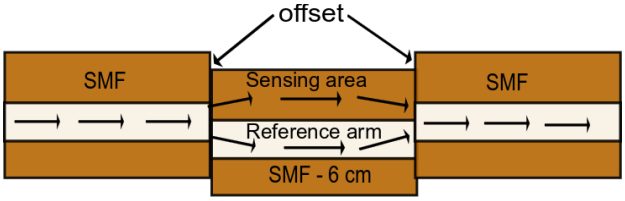

Figure 1 The schematic diagram of a typical Mach-Zehnder interferometer (MZI) by the technique of misalignment of the fiber axes.

ISSN: 2524-2121

CUCHIMAQUE-LUGO, Leidy Johanna, SOSA-MORALES, María Elena,CASTRO-LÓPEZ Rafael, ESTUDILLO-AYALA, Julián Moisés, JAUREGUI-VAZQUEZ, Daniel, HERNANDEZ-GARCÍA, Juan Carlos, SIERRA-HERNANDEZ, Juan Manuel, and ROJAS-LAGUNA,Roberto. Optical method to measure peroxides: A setup for edible oils sensing using a core-offset Mach-Zehnder Interferometer ECORFAN Journal Taiwan. 2017.

Once the single-mode fiber has an effective refractive index difference between the core section n_c = 1.4598 and the coating section n_{cl} = 1.4458, a phase difference can occur through the physical length of the interferometer. Since the fiber used has a core with a diameter of 8 μm and the coating with a diameter of 125 μm, each one will behave as an optical path with different refractive index. Therefore, upon reaching the light beam at the first coupling, it is diffracted by the two optical paths, and then, the core modes and the modes of the coating are returned to the mode of the nucleus at the second junction. By the phase difference and the strips of separation, which are dependent on the wavelength, the optical power transmitted by the interferometer will be maximum at a certain wavelength. The experimental setup used to characterize Mach-Zehnder interferometer as the degradation of edible oils sensor is shown in Figure 2. A semiconductor laser diode (Qphotonics, model QFBGLD-980-500, MI, USA) with a peak centered at 980 nm was used as a source of pumping. The pumping source is connected to the 3.8 m erbium doped fiber (EDF, Thorlabs, model M5-980-125, Newton, New Jersey, USA) using a wavelength division multiplexer (WDM) and the output of the EDF is spliced with the Mach-Zehnder interferometer.

The output power of the sensing setup was monitored by an optical spectrum analyzer (OSA, Yokogawa AQ6370C, Tokyo, Japan) with a resolution of 20 pm.

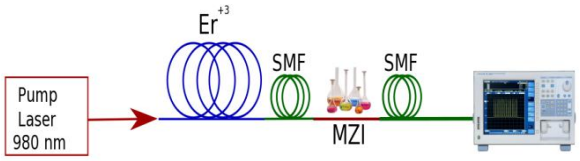

Figure 2 Experimental setup used to characterize Mach-Zehnder interferometer.

Oil samples were obtained from the repeated frying of baked fried foods (Castro-López et al., 2017). The analytical determination of peroxides was done according to the Mexican standard NMX-F-154-SCFI-2010. In a flask, 1 g of KI and 1 g of oil were placed and 30 mL of glacial acetic acid-chloroform solution (3: 2 v/ v) were added. Then, 0.5 mL of 5% KI solution and 30 mL of distilled water were added and heated in a water bath for 1 min. 2.5 ml of 2% starch solution was added and the final solution was titrated with 0.01 N sodium thiosulfate solution until get uncolored solution. Determinations were done by duplicate.

Results

When the fundamental mode being transmitted by the single-mode fiber passes through the first collapse region, the mode is diffracted and a part of the light is coupled to the core section of the SMF. Another part is coupled to the coating section as a result both the core mode and the coating modes are excited. Since both sections have different effective refractive index, a phase difference occurs and as a result, the modes are transmitted at different speeds along the entire section of the MZI.

In addition, when these modes reach the second collapse region, these are reacted back to the single mode fiber. Thus, the two regions of collapse act as optical couplers and the sections of both the core and the cladding act as arms of the interferometer. As a result of the interference between the core mode and the coating mode an interference pattern is obtained as shown in Figures 3 and 4. The separation between two consecutive stripes is given by the equation (1).

$$\Delta\lambda = \lambda^2 / \Delta nL \quad (1)$$

ISSN: 2524-2121

CUCHIMAQUE-LUGO, Leidy Johanna, SOSA-MORALES, María Elena,CASTRO-LÓPEZ Rafael, ESTUDILLO-AYALA, Julián Moisés, JAUREGUI-VAZQUEZ, Daniel, HERNANDEZ-GARCÍA, Juan Carlos, SIERRA-HERNANDEZ, Juan Manuel, and ROJAS-LAGUNA,Roberto. Optical method to measure peroxides: A setup for edible oils sensing using a core-offset Mach-Zehnder Interferometer ECORFAN Journal Taiwan. 2017.

Where λ is wavelength, Δn is the difference of effective refractive indices between the regions of the core and coating of the SMF and L is the length of the interferometer. At this point, it is important to mention that room temperature remained constant, in order to carry out all the experimental characterizations (Huerta-Mascotte et al., 2016).

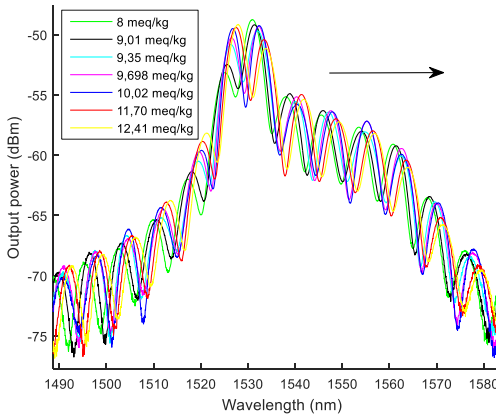

Figure 3 Transmission spectrum in edible oils.

In the Figure 3, the spectral shifting of the MZI, can be observed, under different peroxides indexes of edible oils. Futhermore, in the Figure 4, to determine the spectral changing, can be appreciated that the wavelength moves towards the right for a range from 1540 to 1548 nm.

Finally, Figure 5 was obtained from data shown in Table 1, which in making a linear trend of the corresponding data is obtained a dip of 0.88 corresponding to the sensitivity of the sensor characterized.

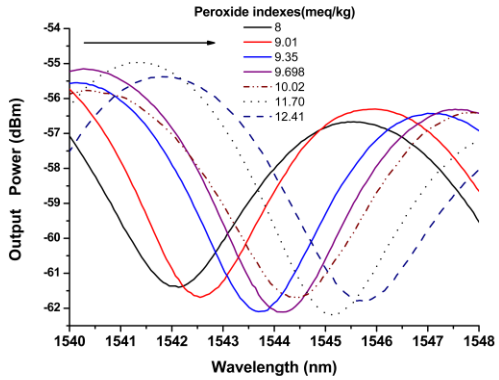

Figure 4 Spectral changing for the range of 1540 nm to 1548nm.

Wavelength(nm)	Peroxide indixes(meq/kg)
1542.037	8
1542.554	9.01
1543.677	9.35
1544.149	9.69
1544.376	10.02
1545.119	11.70
1545.699	12.41

Table 1 Values for wavelength as function of the peroxide indixes.

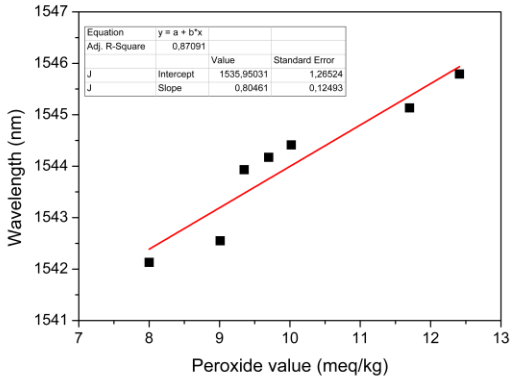

Figure 5 The interference spectrum to dip centered at 1541 nm.

CUCHIMAQUE-LUGO, Leidy Johanna, SOSA-MORALES, María Elena,CASTRO-LÓPEZ Rafael ESTUDILLO-AYALA, Julián Moisés, JAUREGUI-VAZQUEZ, Daniel, HERNANDEZ-GARCÍA, Juan Carlos, SIERRA-HERNANDEZ, Juan Manuel, and ROJAS-LAGUNA,Roberto. Optical method to measure peroxides: A setup for edible oils sensing using a core-offset Mach-Zehnder Interferometer ECORFAN Journal Taiwan. 2017.

ISSN: 2524-2121

Conclusions

A sensing of the degradation in edible oils based on a core-offset Mach-Zehnder interferometer was proposed, based on a 6 cm section of SMF. The output power spectrum shift occurs between wavelengths of 1490-1580 nm with a good linearity in the dynamic range between 8 to 12.41 meq/kg for edible oils with visibility of 7.07 dBm an approximate sensitivity of 0.88 nm/meq/kg in the range of 1540 to 1548 nm. This work is starting and the instrument still needs to be detailed and tested in other range of peroxides.

Acknowledgments

L.J. Cuchimaque-Lugo was supported by the National Council for the Science and Technology (CONACyT) of Mexico for her Master studies and under Project CB-2016-286916.

References

Enríquez-Fernández, B. E., Álvarez de la Cadena y Yañez, L., & Sosa-Morales, M. E. (2012). Influence of Oil Type and Freshness on the Sensory Perception of Fried Foods. *Journal of Culinary Science & Technology* 10(2), pp. 145-153.

Flores-Álvarez, M., Molina-Hernández, E. F., Hernández-Raya, J. C., & Sosa-Morales, M. E. (2012). The Effect of Food Type (Fish Nuggets or French Fries) on Oil Blend Degradation during Repeated Frying. *Journal of Food Science* 77(11), pp. 182 - 190.

NMX-F-154-SCFI-2010. Foods - oils and vegetable fats or animals. Determination of peroxide value-test method. Diario Oficial de la Federación. Mexican Government. (In Spanish).

Li, L., Xia, L., Xie, Z., & Liu, D. (2012). All-fiber Mach-Zehnder interferometers for sensingapplications. *Optics Express* 20(10), pp. 11110.

Zhang, S., Zhang, W., Gao, S., Geng, P., and Xue, X. (2012). Fiber-optic bending vector sensor based on Mach-Zehnder interferometer exploiting lateral-offset and up-taper. *Opt. Lett.* 37(21), pp. 4480–4482.

Duan, D. W., Rao,Y. J., Xu, L. C. Zhu, T. D. Wu, and Yao, J. (2011). In-fiber Mach-Zehnder interferometer formed by large lateral offset fusion splicing for gases refractive index measurement with high sensitivity. *Sens. Actuators B Chem.* 160(1), pp. 1198–1202.

Castro-Lopez R., Gómez-Salazar J.A., Cerón-García A., Sosa-Morales M.E. 2017. Stability of palm olein oil with different antioxidants during repeated frying of churros (Spanish fried dough pastry). CSBE/SCGAB 2017 Annual Conference, 6-10 August, Winnipeg, Manitoba, Canada. Paper No. CSBE17-101.

Huerta-Mascotte, E., Sierra-Hernandez, J. M., Mata-Chavez, R. I., Jauregui-Vazquez, D., Castillo-Guzman, A., Estudillo-Ayala, J. M., … Rojas-Laguna, R. (2016). A Core-Offset Mach Zehnder Interferometer Based on A Non-Zero Dispersion-Shifted Fiber and Its Torsion Sensing Application. *Sensors (Basel, Switzerland)* 16(6), pp. 856. doi:10.3390/s16060856.

ISSN: 2524-2121

CUCHIMAQUE-LUGO, Leidy Johanna, SOSA-MORALES, María Elena,CASTRO-LÓPEZ Rafael, ESTUDILLO-AYALA, Julián Moisés, JAUREGUI-VAZQUEZ, Daniel, HERNANDEZ-GARCÍA, Juan Carlos, SIERRA-HERNANDEZ, Juan Manuel, and ROJAS-LAGUNA,Roberto. Optical method to measure peroxides: A setup for edible oils sensing using a core-offset Mach-Zehnder Interferometer ECORFAN Journal Taiwan. 2017.

Article **ECORFAN-Journal**
December 2017 Vol.1 No.2 11-15

Detecting glucose levels by means of Raman spectroscopy, support vector machine and principal component analysis

CASTRO-RAMOS, J.[†]*, VILLA-MANRÍQUEZ, J. F.[†], GÓMEZ-GIL, P.[†], GONZÁLEZ-VIVEROS, N.[†], NAREA-JIMÉNEZ, F.[†], SÁNCHEZ-ESCOBAR J. J.[††] and MUÑOZ-LÓPEZ, J.[†]

[†] *Instituto Nacional de Astrofísica Óptica y Electrónica, Luis Enrique Erro 1, Tonantzintla, Puebla, México, C.P. 72000.*
[††] *Centro de Enseñanza Técnica Industrial, Nueva Escocia 1885 Fraccionamiento Providencia, Guadalajara, Jalisco, México, C. P. 44620.*

Received September 21,2017; Aceppted November 21, 2017

Abstract

In this paper we present the results of automatically detecting the glucose levels in chemical solutions. We prepared a set of different solutions, each with different concentrations of anhydrous glucose, which was increased by 10% with respect to the previous one; these dissolutions were diluted in water. Using the whole Raman spectra as features representing the samples, and principal component analysis with support vector machines as a classification method, we predicted the concentration level, getting an accuracy of classification of 79.16% measured using AUC (Area Under the ROC) Curve.

Glucose Level Solution, Raman Spectroscopy, PCA, SVM

Citation: CASTRO-RAMOS, J[†] *, VILLA-MANRÍQUEZ, J F, GÓMEZ-GIL, P, GONZÁLEZ-VIVEROS, N, NAREA-JIMÉNEZ, F, SÁNCHEZ-ESCOBAR J J[†] and MUÑOZ-LÓPEZ, J. Detecting glucose levels by means of Raman spectroscopy, support vector machine and principal component analysis. ECORFAN Journal Taiwan. 2017, 1-2: 11-15

*Correspondance to Author (email: jcastro@inaoep.mx

Introduction

Diabetes mellitus is an important health problem diagnosed whether glucose level is greater than 126 mg/ml. nowadays almost all commercial methods to detect either the level of glucose or glycosylated haemoglobin in humans are invasive. A huge quantity of devices measuring levels of glucose require a drop of blood, which is obtained through a puncture with a needle; it is painful and in some cases traumatic.

In the other hand, it is possible that people living in developing countries does not check their glucose levels due to cost of clinical analysis are high.Several studies have been reported before, using Raman espectergrapy for measuring glucose. For example, Wei Gao et al. (2016), worked on a noninvasive device, which measures sweat metabolites such as glucose, lactate and electrolytes.

Barman et al. (2010), developed a model for monitoring blood glucose using Support Vector Machines and Raman Spectroscopy; the authors showed the nonlinear effects in the relationship between the concentrations of the solute of interest and the mixture Raman spectra. Prominent Raman bands associated with glucose (926, 1302, 1125 cm^{-1}) were mention by Zephania Birech et al. (2017), likewise Jingwei Shao et al (2012), mention 796, 1060, 1125 and 1366 like Raman bands. In the work of Mircea Oroian et al. (2017) Raman spectroscopy is used to detect honey adulterated with fructose, and other substances.

In this paper we present a non-invasive method to quantify the levels of glucose from several levels of concentration. The proposed method is based on Raman spectroscopy, principal component analysis and support vector machine.

It is important to point out that in a previous work Villa-Manríquez et al. (2017) applied a similar method was successfully applied to detect the glycated hemoglobin in vivo, without the need for blood. In such work we showed the capability of the method to distinguish between diabetic and non-diabetic patients.

Raman spectroscopy

The Raman Effect or Raman scattering was discovered by Chandrasekara Venkata (1928), Raman Effect is inelastic; the energy of photons scattered from a sample are either higher or lower than the energy of the incident light. There is a type of vibrational spectroscopy that measures the fundamental vibrational modes of chemical bonds and it is used to generate molecular specific information about a sample Colthup et al (1990), thereby it allows the detection of molecular bonds of glucose.

Principal Component Analysis and Support vector Machine

Support vector machines (SVMs) is a discriminative and supervised method, with associated learning algorithms that analyzes data. It is used for classification and regression analysis which is done finding a separating hyperplane.

Principal component analysis (PCA) is a statistical procedure, used to reduce the dimensionality of a data set. It is formed by a large number of interrelated variables. An orthogonal transformation converts a set of observations into a set of values of linearly uncorrelated variables, called principal components.

ISSN: 2524-2121

Methodology

We prepared the samples by dissolving anhydrous glucose in distilled water. We got a set of samples, each with a different concentration with differences of 10% each.

We used the mass concentration definition, it means the constituent in gr (mass), is divided by the mixture in liter (volume). Samples were put in cuvettes. A test probe was placed at the top of the container to acquire Raman signal. We use the experimental setup shown in Figure 1.

We used PCA, to get principal components which are used as features to input to the classifier. The use of PCA allows to reduce the dimension of the data, without losing relevant information. It is important to point out that the complete Raman spectra was used for calculating the principal components.

The reduced features were used for SVM training, with K-fold cross-validation iterations, that is, data was divided into K subsets (folds). One of the subsets was used as a test set and the rest (K-1 folds) as training set. The cross-validation process was repeated for K iterations, using each of the available subsets of test data, with K = 10.

The error was calculated as the arithmetic mean of the errors of each iteration. The average obtained accuracy was 79.16%, wich was obtained using an SVM with a quadratic kernel, implemented in the statistical programming language R (2016).

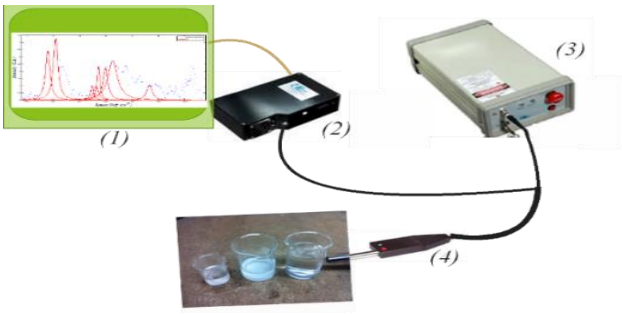

Figure 1. Experimental setup: (1) the computer monitor, (2) the Raman spectrometer, (3) the excitation light source, (4) the sample measurement of Raman spectra.

Results

Figure 2, shows the Raman spectra of samples at different concentrations in a range from 900 to 1200 cm^{-1}.

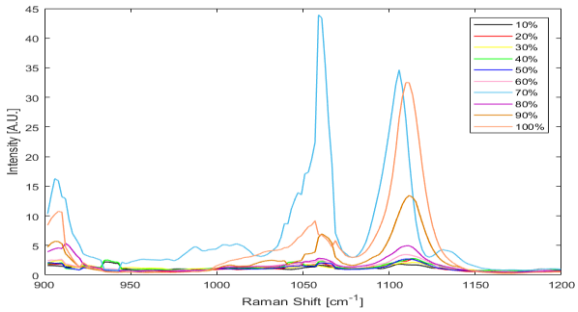

Figure 2. Raman spectra of different solutions with concentrations from 10 to 100 %.

Figure 3 a), shows a map of the decision regions. In that we can differentiate between each concentration, hence it is possible to classify these samples using PCA and SVM. Classification results are shown in figure 3 b). Notice that class labeled "30%" was not well classified (see figure 4 b, the confusion matrix), due to systematic errors in measurements. In future work we will take more measurements to see if this issue is corrected.

ISSN: 2524-2121

a)

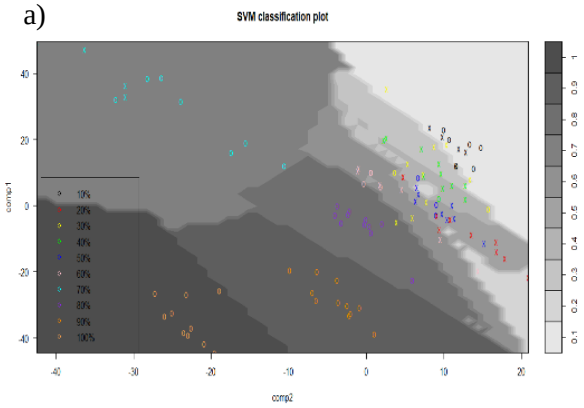

b)

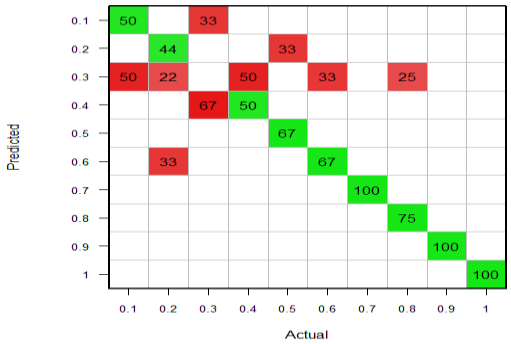

Figure 3. (a) SVM and PCA results, (b) confusion matrix

Conclusions

We analysed the results of a method to quantify glucose in dissolutions, using PCA-SVM, which was tested using k-fold cross validation. We found quadratic kernel results to be a good method to select the optimum level of glucose from the set of trained samples used in this experiment.

Still, more experiments are required, but this results are promising and therefore this method could be applied to know the presence of different concentrations of glucose, considering that in average it was found a classification accuracy of 80%.

Our final goal is to apply automatic classification for measuring glucose in blood.

References

GAO, W., Emaminejad, S., Hnin Yin Yin Nyein, Challa, S., Chen, K., Peck, A., Fahad, H. M., Ota, H., Shiraki, H., Kiriya, D., Lien, D.-H., Brooks, G. A. (2016). Fully integrated wearable sensor arrays for multiplexed in situ perspiration analysis. *Nature* 529, pp. 509–514

Barman, I., Kong, C.-R., Dingari, N. C., Dasari, R. R. and Feld, M. S. (2010). Development of Robust Calibration Models Using Support Vector Machines for Spectroscopic Monitoring of Blood Glucose. *Analytical Chemistry* **82**(23), pp. 9719–9726.

Birech, Z., Mwangi, P. W., Bukachi, F., & Mandela, K. M. (2017). Application of Raman spectroscopy in type 2 diabetes screening in blood using leucine and isoleucine amino-acids as biomarkers and in comparative anti-diabetic drugs efficacy studies. *PLoS ONE*, *12*(9), 1–12. https://doi.org/10.1371/journal.pone.0185130

Shao, J., Lin, M., Li, Y., Li, X., Liu, J., Liang, J., & Yao, H. (2012). In Vivo Blood Glucose Quantification Using Raman Spectroscopy. *PLoS ONE*, *7*(10), 1–6. https://doi.org/10.1371/journal.pone.0048127.

Oroian, M., Ropciuc, S., & Paduret, S. (2017). Honey Adulteration Detection Using Raman Spectroscopy, (July).

Villa-Manríquez, J. F. Castro-Ramos, J., Gutiérrez-Delgado, F., Lopéz-Pacheco, M. A. and Villanueva-Luna, A. E. (2017). Raman spectroscopy and PCA-SVM as a non-invasive diagnostic tool to identify and classify qualitatively glycated hemoglobin levels in vivo. *Journal of Biophotonics* 10(8), pp. 1074-1079.

ISSN: 2524-2121

C. V. Raman & K. S. Krishnan, A New Type of Secondary Radiation, (1928), Nature 121, 501–502.

Colthup, N. B. Daly, L. H., Wiberley, S. E. (1990). Introduction to infrared and Raman spectroscopy. Academic Press, Inc.R Core Team (2016). R: A language and environment for statistical computing. R

Foundation for Statistical Computing, Vienna, Austria. https://www.R-project.org/

ISSN: 2524-2121

Article **ECORFAN-Journal**
December 2017 Vol.1 No.2 16-21

Sugar concentration sensor based on a micro Fabry-Perot interferometer

GUZMAN-CHAVEZ, Ana Dinora†[,], CANO-CONTRERAS, Martín[,,] and JAUREGUI-VAZQUEZ, Daniel[,,,]

[,] *Universidad de Guanajuato, Departamento de Estudios Multidisciplinarios, Divisón de Ingenierías, Av. Universidad s/n, Col. Yacatitas, Yuriria, Guanajuato, México, C.P. 38940.*

[,,] *Universidad Tecnológica del Suroeste de Guanajuato, Departamento de Tecnologías de la Información y Comunicación, Carr. Valle-Huanímaro km. 1.2. Valle de Santiago, Gto. C. P. 38400.*

[,,,] *Universidad de Guanajuato, Departamento de Ingeniería Electrónica, División de Ingenierías, Campus Irapuato-Salamanca, , Comunidad de Palo Blanco, Salamanca, Gto., C.P. 36885, México.*

Received September 30, 2017; Accepted December 12, 2017

Abstract

In this work a fiber optic sensor based on a micro Fabry-Perot interferometer (MFPI) for measuring sugar concentration in distilled water is presented. Here the spectral fringes contrast of the MFPI decreases when the refractive index value that surrounds it increases. As each sugar solution has a specific refractive index value, it was possible to relate the sugar concentration of aqueous solutions by measuring the power reflected of one MFPI spectral fringe. Moreover the sensor response to refractive index changes is modelled by using the characteristic matrix method. Finally this sensing arrangement for measuring sugar concentrations achieved a sensitivity of -0.0123 dBm/(gr/100ml) for the measurement range from 0 to 30.88 gr/100 ml at 1538.27 nm wavelength.

Fabry-Perot Interferometer, Sugar Concentration, Refractive Index

Citation: GUZMAN-CHAVEZ, Ana Dinora†, CANO-CONTRERAS, Martín and JAUREGUI-VAZQUEZ, Daniel. Sugar concentration sensor based on a micro Fabry-Perot interferometer. ECORFAN Journal Taiwan. 2017, 1-2: 16-21

*Correspondance to Author (email: jchernandez@ugto.mx)
† Researcher contributing as first author.

Introduction

Humans have been consuming sugar for many centuries. This product is one of the main ingredients to give sweetness to foods and beverages (Yusmawati et al., 2007). Therefore there are many producers of sugar and products that contain it. The production of sugar is accomplished by a variety of processes in the plants, making indispensable the development of efficient measurement techniques for the improvement of the process control and to preserve the quality of final products. Some traditional methods to measure sugar content are based on refractive index measurement of the solution. These methods are mainly based on a bulky prisms system (Dorn & Wolf, 1970). In recent years new techniques, based on fiber optic sensor to measure refractive index, have been developed.

These fiber sensors offer the advantages such a as immunity to electromagnetic interference, small size, capability of in-situ, and real time applications. Recently, a variety of fiber optic sensor to measure solute concentration of aqueous solutions have been reported, some of these sensors are based on: long period gratings (Chong et al., 2006; Jorge et al., 2012), modulated path optical fiber (Marzuki, Wulan & Riatun, 2016), Fresnel reflection from the tip of a fiber (Binu et al., 2009; Chang-Bong, 2003; Fujiwara, Ono, Manfrim, Santos & Suzuki, 2011), and a fiber removed portion (Guzman-Sepulveda et al., 2013; Jayanth Kumar et al., 2006).

In this work a sugar concentration sensing setup based on a micro Fabry-Perot interferometer is presented. Here the sensor head is a MFPI that is in the tip of a single mode fiber (SMF). The MFPI is a micro bubble fabricated with a segment of hollow core photonic crystal fiber.

Its reflected interference pattern can be modified when solution refractive index that surrounds it changes. These refractive index values can be obtained by changing sugar concentration in water distilled. In this sense the fringes contrast of the MFPI reflected pattern decreases when sugar concentration increases. Therefore it was possible to calculate sugar concentration of aqueous solutions by measuring the reflected power of the spectral fringes. Experimental sugar concentrations measurements within the range from 0 to 30.88 gr/100 ml are provided. Finally the sensor response to refractive index changes is modelled by using the characteristic matrix method.

Methodology

The proposed setup for measuring sugar concentration is shown in Figure 1. Here, the light of a pigtailed diode laser emitting at 980 nm, delivering a maximum output power of 200 mW, was coupled to a wavelength division multiplexer to pump an erbium doped fiber (Newport F-EDF-T3) of 3.4 m length.

Afterwards, the luminescence generated by the EDF travels toward the FPI through the circulator from the port 1 to the port 2. Finally, the reflected interference spectrum of the FPI was monitored at the port 3 of the circulator by using an optical spectrum analyser (OSA, Yokogawa AQ6370C) with a resolution of 0.02 nm.

In order to measure sugar concentration changes, the FPI was placed into a cuvette which was filled with different sugar solutions. In this arrangement the sensor head is the intrinsic MFPI which is based on an air microcavity. This was fabricated by splicing a segment of hollow core photonic crystal fiber (HC-1064-19 Cells Fiber Crystal) to a standard SMF.

ISSN: 2524-2121

Here to splice both fibers a conventional arc fusion splicer (Fitel-S175) was used and the fabrication process described in detail by (Jauregui-Vazquez et al., 2013) was followed. In this process after fibres get spliced multiple electric discharges are applied in order to cleave the photonic crystal fiber. After this step an air microcavity (MFPI) at the tip of the SMF is obtained (Figure 2). The sensor head is a MFPI which is considered like a structure of two plane and parallel plates. The first plate is the microcavity with length d_1 with a refractive index n_1 and the second plate is the thin silica wall at the tip of the FPI with thickness d_2 with a refractive index n_2. The incident medium of the pile of plates is the SMF core, with a refractive index n_2, and the exit medium that will depend on the material surrounding the MFPI structure, has a refractive index n_e. For this structure as both plates have low reflectivity therefore only two main interference spectra will occur. The first interference spectrum will be generated within the air micro cavity while the second one will occur within the thin silica wall.

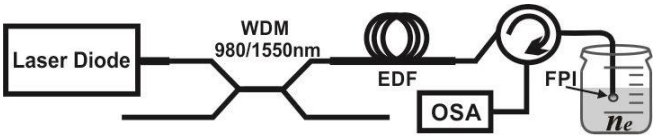

Figure 1. Sugar concentration sensing setup

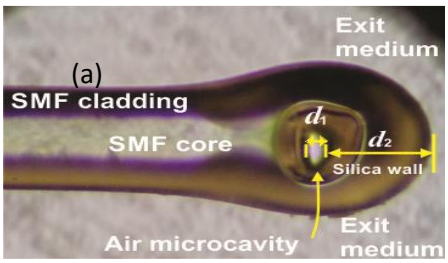

Figure 2. Picture of the fabricated MFPI.

Hence, as the overall MFPI is seen as a pile of plates therefore the final MFPI reflectivity fringe pattern can be calculated by using the characteristic matrix (Dorn & Wolf, 1970). Then the reflectance of this plate assembly can be obtained by using the following expression (Vargas-Rodriguez et al., 2015):

$$\begin{bmatrix} A \\ B \end{bmatrix} = \begin{bmatrix} \cos\delta & -\frac{1}{n_1}\sin\delta \\ in_1 \sin\delta & \cos\delta \end{bmatrix} \begin{bmatrix} \cos\delta & -\frac{i}{n_2}\sin\delta \\ in_2 \sin\delta & \cos\delta \end{bmatrix} \begin{bmatrix} 1 \\ n_e \end{bmatrix} \quad (1)$$

$$\delta = \frac{2\pi n_{1,2} d_{1,2}}{\lambda} \quad (2)$$

where λ is the wavelength. Finally the reflectivity of the overall assembly is given by:

$$R_{FPI} = real\left(\frac{n_2 A - B}{n_2 A + B}\right)^2 + imag\left(\frac{n_2 A - B}{n_2 A + B}\right)^2 \quad (3)$$

In order to simulate our system response, we considered $d_1 = 12.7\ \mu m$, $d_2 = 110.9\ \mu m$, $n_1 = 1$, $n_2 = 1.44$. Simulated reflectivity spectra of the MFPI for three different n_e are shown in Fig. 3. Here, it can be appreciated that in this type of MFPI the contrast and the finesse of the spectral fringes occurring by multiple internal reflections within the second plate (the thin silica wall) will be modified (Fig. 3b).

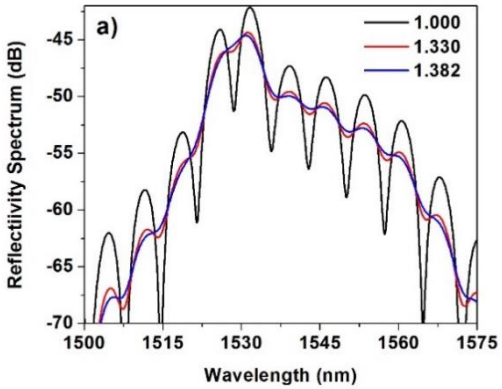

Figure 3. a) Simulated MFPI reflectivity spectra considering an exit medium with different refractive indexes. b) Detail of the FPI reflectivity spectra.

ISSN: 2524-2121

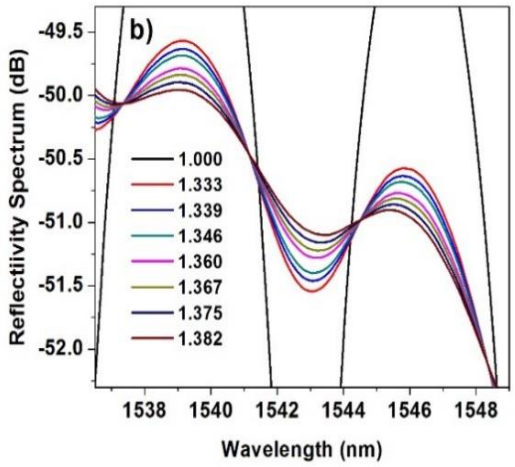

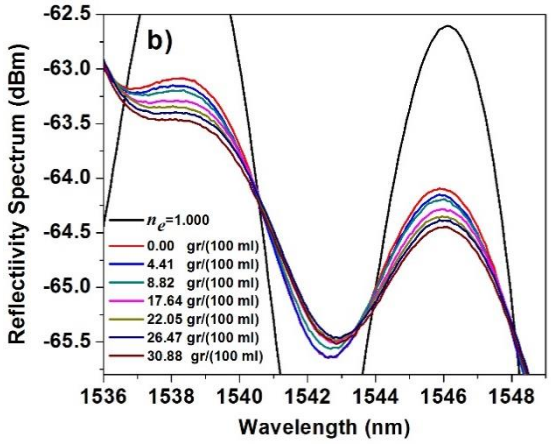

Figure 4. a) Measured reflected power spectra for different values of sugar concentrations and a b) Detail of the spectra.

Sugar Concentration Sensor Response

The measured MFPI reflection profiles for two different sugar concentrations are shown in Figure 4a. Here the sugar concentrations were prepared using table sugar or granulated sugar and distilled water. The sugar concentrations that we used to characterize the sensor response were from 0 gr/100 ml to 30.88 0 gr/100 ml that correspond to the refractive indexes from 1.333 to 1.382 RIU respectively. In fig. 4b a detail of the spectral profiles for these sugar solutions are presented.

It can be observed that the contrast of the spectral fringe decreases when the refractive index of the sugar solution increases, related with the increase in sugar concentration. This behavior is predicted by the simulated results.

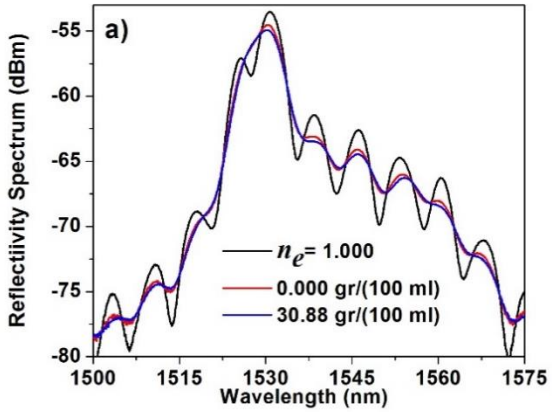

As the contrast of the spectral fringes changes as the sugar concentration of the exit medium is varied, therefore it is possible to detect these changes by measuring the amount of reflected light at certain wavelength.

For instance, we select the maximum of one fringe, which in our case occur at $\lambda = 1538.27$ nm (Fig.4b). Moreover, the reflected energy, in dBm, as a function of the sugar concentration and the refractive index is presented in Figure 5. It can be noticed that the reflected light by the MFPI at $\lambda = 1538.27$ nm can be fitted very well with a linear function. The linearity has a correlation coefficient of 0.998.

Moreover, from these measurements it is possible to determine that the sensor has a sensitivity of -7.75 dBm/RIU or -0.0123 dBm (100 ml)/gr. Finally it is important to mention that measurements were taken directly with the OSA, however for practical reasons it must be replaced by a simple optical stage and low cost photodetectors (Vargas-Rodriguez et al., 2015).

ISSN: 2524-2121

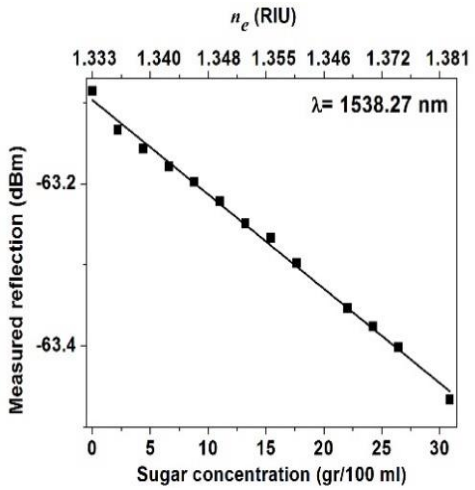

Figure 5. Measured reflected energy at $\lambda = 1538.27$ nm as a function of the sugar concentration and the exit medium refractive index

Conclusions

In this work a fiber optic sensor based on a micro Fabry-Perot interferometer (MFPI) for measuring sugar concentration in distilled water was presented. Here it was shown that the spectral fringes contrast of the MFPI decreased when the refractive index value that surrounds it increased.

As each sugar solution has a specific refractive index value, it was possible to relate the sugar concentration of aqueous solutions by measuring the power reflected of one MFPI spectral fringe. Moreover the sensor response to refractive index changes was modelled by using the characteristic matrix method.

Finally this sensing arrangement for measuring sugar concentrations achieved a sensitivity of -0.0123 dBm/(gr/100ml) for the measurement range from 0 to 30.88 gr/100 ml at 1538.27 nm wavelength

References

Yusmawati, W.Y.W., Chuah, H.P., & Mahmood, M.Y.W. (2007). Optical properties and sugar content determination of commercial carbonated drinks using surface plasmon resonance. *American Journal of Applied Sciences* **4**(1), pp. 1–4.

Dorn, M., & Wolf, E. (1970). Principles of Optics. Pergamon Press: Oxford, UK.

Chong, J.H., Shum, P., Haryono, H., Yohana, A., Rao, M.K., Lu, C., & Zhu, Y. (2003). Measurements of refractive index sensitivity using long-period grating refractometer. *Optics Communications* **229**(1–6), pp. 65–69.

Jorge, P.A.S., Silva, S.O., Gouveia, C., Tafulo, T., Coelho, L., Caldas, P., Viegas, D., Rego, G., Baptista, J.M., Santos, J.L., & Orlando, F. (2012). Fiber optic-based refractive index sensing at INESC Porto. *Sensors* **12**(6), pp. 8371–8389.

Marzuki, A., Wulan Sari, N., & Riatun (2016). Design of reflective optical fiber sensor for determining refractive index and sugar concentration of aqueous solutions. 10th Joint Conference on Chemistry, 012032.

Binu, S., Mahadevan Pillai, V.O., Pradeepkumar, V., Padhy, B.B., Joseph, C.S., & Chandrasekaran, N. (2009). Fibre optic glucose sensor. *Materials Science and Engineering: C* 29(1), pp. 183-186.

Chang-Bong, K. (2003). A Fiber Optic sensor measurements of solute concentrations in fluids. *Journal of the Optical Society of Korea* **7**(2), pp. 102-105.

ISSN: 2524-2121

Fujiwara, E., Ono, E., Manfrim, T.P., Santos, J.S., & Suzuki, C.K. (2011). Measurement of sucrose and ethanol concentrations in process streams and effluents of sugarcane bioethanol industry by optical fiber sensor. *Proceeding of SPIE*. 7753, 775351-4.

Guzman-Sepulveda, J.R., Ruiz-Perez, V.I., Torres-Cisneros, M., Sanchez-Mondragon, J.J., & May-Arrioja, A. (2013). Fiber Optic Sensor for High-Sensitivity Salinity Measurement. *IEEE Photonics Technology Letters* 25(23), pp. 2323-2326.

Jayanth Kumar, A., Gowri, N.M., Venkateswara Raju, R., Nirmala, G., Bellubbi, B.S., & Radha Krishna, T. (2006). Study of fiber optic sugar sensor. *PRAMANA-Journal of Physics* 67(2), pp. 383-387.

Jauregui-Vazquez, D., Estudillo-Ayala, J.M., Rojas-Laguna, R., Vargas-Rodriguez, E., Sierra-Hernandez, J.M., Hernandez-Garcia, J.C., & Mata-Chavez, R.I. (2013). An all fiber intrinsic Fabry-Perot interferometer based on an air-microcavity. *Sensors* 13, pp. 6355–6364.

Vargas-Rodriguez, E., Guzman-Chavez, A.D., Cano-Contreras, M., Gallegos-Arellano, E., Jauregui-Vazquez, D., Hernandez-Garcia, J.C., Estudillo-Ayala, J.M., & Rojas-Laguna, R. (2015). Analytical Modelling of a Refractive Index Sensor Based on an Intrinsic Micro Fabry-Perot Interferometer. *Sensors* 15, pp. 26128-26142.

ISSN: 2524-2121

Instructions for authors

A. Submission of papers to the areas of analysis and modeling problems of the current international society.

B.The edition of the paper should meet the following characteristics:

-Written in English. It is mandatory to submit the title and abstract as well as keywords.Indicating the institution of affiliation of each author, email and full postal address and identify the researcher and the first author is responsible for communication to the editor

-Print text in Times New Roman #12 (shares-Bold) and italic (subtitles-Bold) # 12 (text) and #9 (in quotes foot notes), justified in Word format. With margins 2 cm by 2 cm left-right and 2 cm by 2 cm Top-Bottom. With 2-column format.

-Use Calibre Math typography (in equations), with subsequent numbering and alignment right: Example;

$$σϵ∑:Hσ=⋂\_(s<σ)Hs \quad (1)$$

-Start with an introduction that explains the issue and end with a concluding section.

- Items are reviewed by members of the Editorial Committee and two anonymous. The ruling is final in all cases. After notification of the acceptance or rejection of a job, final acceptance will besubject to compliance with changes in style, form and content that the publisher has informed the authors. The authors are responsible for the content of the work and the correct use of the references cited in them. The journal reserves the right to make editorial changes required to adapt the text to our editorial policy.

C.Items can be prepared by self or sponsored by educational institutions and business. The manuscript assessment process will comprise no more than twenty days from the date of receipt.

D.The identification of authorship should appear in a first page only removable in order to ensure that the selection process is anonymous.

E.Charts, graphs and figures support must meet the following:

-Should be self-explanatory (without resorting to text forunderstanding), not including abbreviations, clearly indicating the title and reference source with reference down with left alignment number 9 with bold typography.

-All materials will support gray scale and maximum size of 8 cm wide by 23 cm tall or less size, and contain all content editable.

- Tables should be simple and present relevant information. Prototype;

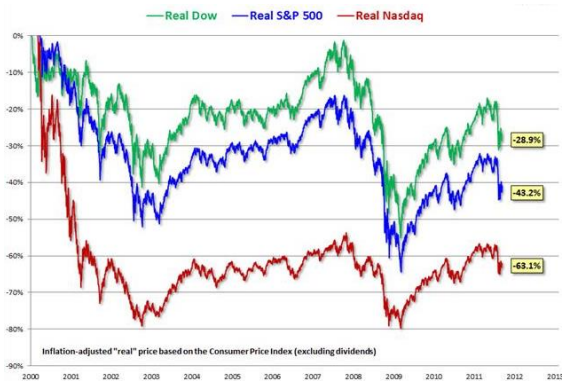

Graph 1. Three "Real" Indexes: Percent change from Their 2000 Peaks

F. References are included at the end of the document, all its components will be separated by a comma and must the following order:

- Articles: Kejun, Z. (2012). Feedback Control Methods for a New Hyperchaotic System. Journal of Information & Computational Science, No.9. Pp :231-237.

- Books: Barnsley, M. (1993). Fractals Everywhere. Academic Press. San Diego.

- WEB Resources: http://www.worldfederationofexchanges.com, see: (August, 16-2012)

The list of references should correspond to the citations in the document.

G. The notes to footnotes, which should be used and only to provide essential information.

H. Upon acceptance of the article in its final version, the magazine tests sent to the author for review. ECORFAN only accept the correction of typos and errors or omissions from the process of editing the journal fully reserving copyright and dissemination of content. Not acceptable deletions, substitutions or additions which alter the formation of the article. The author will have a maximum of 10 calendar days for the review. Otherwise, it is considered that the author (s) is (are) in accordance with the changes made.

I.Append formats Originality and Authorization, identifying the article, author (s) and the signature, so it is understood that this article is not running for simultaneous publication in other journals or publishing organs.

Taiwan ____ , ____ 20_____

Originality Format

I understand and agree that the results are final dictamination so authors must sign before starting the peer review process to claim originality of the next work.

Article

_____

Signature

_____

Name

Taiwan ____ , ____ 20_____

Authorization form

I understand and accept that the results of evaluation are inappealable. If my article is accepted for publication, I authorize ECORFAN to reproduce it in electronic data bases, reprints, anthologies or any other media in order to reach a wider audience.

_____

Article

_____

Signature

_____

Name

ECORFAN Journal-Republic of Taiwán

Optical characterization of nanostructured Opal-C
DURÁN-MUÑOZ, H.A., SIFUENTES-GALLARDO, C., HERNÁNDEZ-ORTIZ, M., DÍAZ-CARRILLO, C., ULLOA-CAMPOS, M., ORTIZ-HERNÁNDEZ, A. and GUTIÉRREZ-ALMARAZ G.
Universidad Autónoma de Zacatecas
Universidad Politécnica de Zacatecas

Optical method to measure peroxides: A setup for edible oils sensing using a core-offset Mach-Zehnder Interferometer
CUCHIMAQUE-LUGO, Leidy Johanna, SOSA-MORALES, María Elena, CASTRO-LÓPEZ Rafael, ESTUDILLO-AYALA, Julián Moisés, JAUREGUI-VAZQUEZ, Daniel, HERNANDEZ-GARCÍA, Juan Carlos, SIERRA-HERNANDEZ, Juan Manuel, and ROJAS-LAGUNA, Roberto
Universidad de Guanajuato

Detecting glucose levels by means of Raman spectroscopy, support vector machine and principal component analysis
CASTRO-RAMOS, J., VILLA-MANRÍQUEZ, J. F., GÓMEZ-GIL, P., GONZÁLEZ-VIVEROS, N., NAREA-JIMÉNEZ, F., SÁNCHEZ-ESCOBAR J. J., and MUÑOZ-LÓPEZ, J.
Instituto Nacional de Astrofísica Óptica y Electrónica
Centro de Enseñanza Técnica Industrial

Sugar concentration sensor based on a micro Fabry-Perot interferometer
GUZMAN-CHAVEZ, Ana Dinora, CANO-CONTRERAS, Martín and JAUREGUI-VAZQUEZ, Daniel
Universidad de Guanajuato
Universidad Tecnológica del Suroeste de Guanajuato

2524 2121
ISSN 2524-2121

www.ecorfan.org